

PERTURBATION MAPS FOR A SPACECRAFT AROUND THE NEAR-EARTH ASTEROID (153591) 2001 SN₂₆₃

Diogo M. Sanchez*, Antonio F. B. A. Prado†

The Aster mission is the first Brazilian deep space mission. The target is the triple near-Earth Asteroid 2001 SN₂₆₃. In this work we use the method of the integral of the disturbing accelerations to generate perturbation maps of this system. These maps are used to find less disturbed regions in this asteroid system, and to provide the fuel consumption, in terms of delta-v, to keep a spacecraft as close as possible to a Keplerian orbit. The results of this work can be used for the planning of the Aster mission.

INTRODUCTION

The near-Earth Asteroid 2001SN₂₆₃ is the target of the Aster mission, the first Brazilian deep space mission.¹ This asteroid is actually a triple system, comprised by a central body Alpha and two asteroidal moons, being the inner one Gamma and the outer one Beta. The masses of Alpha, Gamma, and Beta are, respectively, 917.47×10^{10} kg, 9.78×10^{10} kg, and 24.04×10^{10} kg.^{2,3} The semi-major axis of Gamma and Beta are 3.80 km and 16.63 km, respectively. Both Gamma and Beta are almost in circular orbits around Alpha. However, the eccentricity of the system around the Sun is 0.48, with semi-major axis equal to 1.99 au (where 1 au = $1.49597870700 \times 10^8$ km).

Although the Aster mission has started as a project in 2010, this multi-institutional mission still is in its earlier phase of planning. Currently, only the target of the mission was chosen, and the choice of the type of orbit around the asteroid and instruments that the spacecraft will carry is still open. Probably the spacecraft for this mission will be small sized, with maximum mass around 150 kg, to be placed as secondary payload in a contracted launcher also to be defined. Due to the small size of the spacecraft, and the possibility of use of large solar panels to power it, the solar radiation pressure will play an important role in the mission. This effect will become even more important when the system passes by its perihelion, at 1.03 au.

Several studies have been made considering the stability of particles or spacecraft in this system, as we can find, for instance, in References 4 and 5. However, these studies consider the stability from the point of view of survival times of the spacecraft in this system, as well as the maximum eccentricity achieved during these orbits. In particular, the two mentioned studies do not consider the effects of the solar radiation pressure and, as mentioned before, this is an important perturbation that acts over a spacecraft in this system.

*Post-doctoral Fellow, Division of Space Mechanics and Control, National Institute for Space Research - INPE, 12227-010 São José dos Campos, Brazil

†President of the Board of the Graduate School at INPE in Brazil, National Institute for Space Research - INPE, 12227-010 São José dos Campos, Brazil

In this work we propose a new approach to assess, at once, a quantitative measurement of the main perturbations in the system and the delta-v required to keep the spacecraft in a less disturbed orbit: perturbation maps. These maps are grids of initial conditions in which each point of the map is the average velocity applied over the spacecraft by the disturbers, calculated by the method of the integral of the disturbing accelerations (PI method)⁶⁻⁸ after a numerical integration of the equations of motion of all bodies of this system, as well as the disturbing bodies, during a period of integration T . The perturbation maps also can show a qualitative assessment of the the stability of a spacecraft in this system. This qualitative analysis is made by using the perturbation maps of type II, which shows the regions in the system where the disturbers take or add energy to the spacecraft, whereas the quantitative analysis of the less disturbed orbits is made by using the type IV, which measures how much the orbit of the spacecraft deviates from a Keplerian orbit of reference. There are four types of perturbation maps, based on the four types of integrals in the PI method, as we will explain in the next section, but we will use only types II and IV in this work.

As mentioned before, the mass of the spacecraft probably will be equal to 150 kg. Then, we fixed two values for the mean area-to-mass (A/m) ratio of the spacecraft, 0.02 m²/kg and 0.15 m²/kg. We also analyzed the difference between direct and retrograde orbits. Regions where direct orbits are unstable and retrograde orbits are apparently stable are good regions to place the spacecraft, since there are no natural particles present. Among these regions, we will search for the ones with minimum deviation from a Keplerian orbit, because these orbits need less fuel consumption to control the orbit of the spacecraft. The results found in this work can be used in the Aster mission to find a set of orbits around Alpha that can be used for the exploration of the system by a spacecraft.

MATHEMATICAL MODEL AND METHODOLOGY

In this section, the numerical model for the spacecraft and the remaining bodies of the system, as well as the disturbers, is described. It is also described the four types of the method of the integral of the disturbing accelerations (PI method) and the construction of the perturbation maps.

Numerical Method

The model for the motion of the spacecraft in the system is such that the spacecraft has free motion around the entire system, until the limit of 180 km from Alpha, which is the Hill's radius of Alpha. It is considered the perturbation coming from the Sun, Earth, Mars, and Jupiter, as well as the solar radiation pressure with eclipses by Alpha.⁹ It is also taken into account the perturbation from the irregular shape of the central body Alpha, using a spherical harmonics expansion up to order and degree four. Then, the equation of motion of the spacecraft is given by:

$$\ddot{\mathbf{r}} = -\frac{GM_\alpha}{|\mathbf{r}|^3}\mathbf{r} + G \sum_{j=1}^{N-1} M_j \left(\frac{\mathbf{r}_j - \mathbf{r}}{|\mathbf{r}_j - \mathbf{r}|^3} - \frac{\mathbf{r}_j}{|\mathbf{r}_j|^3} \right) + \mathbf{P}_\alpha + \mathbf{P}_{SRP}, \quad (1)$$

where G is the universal gravitational constant, M_α , M_j , and \mathbf{r}_j are the mass of Alpha and the masses and position vectors of the disturbers (Beta, Gamma, Earth, Mars, Jupiter, and the Sun), respectively. \mathbf{r} is the position vector of the spacecraft. The reference system is centered in Alpha, with a reference frame in the "equator" of Alpha, at the reference Epoch. \mathbf{P}_α is the acceleration due to the gravitational potential of Alpha, expanded in spherical harmonics up to order and degree four. This potential is calculated using a modified recursive model given by Reference 10, adapted to Alpha. The adaptations were necessary because this model was originally defined for the Earth,

and it depends on the Greenwich Sidereal Time (GST), which only makes sense for the Earth. In the case of Alpha, we define an angle that works as a pseudo GST and simulates the rotation of Alpha. We also consider Alpha as an homogeneous triaxial ellipsoid. In this case, all odd coefficients of the spherical harmonics expansion are equal to zero. Thus, the remaining coefficients of the spherical harmonics expansion up to degree and order four are given by:¹¹

$$\begin{aligned}
C_{20} &= 0.2155612244897959 \times 10^{-1}, \\
C_{22} &= 0.3507653061224490 \times 10^{-2}, \\
C_{40} &= 0.1048443589352651 \times 10^{-2}, \\
C_{42} &= 0.5400814206878087 \times 10^{-4}, \\
C_{44} &= 0.2197076785342417 \times 10^{-5}.
\end{aligned} \tag{2}$$

These coefficients were calculated using $a = 1.4$ km, $b = 1.35$ km, and $c = 1.45$ km as the semi-axis the of shape of Alpha.³ The coefficients were normalized for the use in the calculation of the potential of Alpha. \mathbf{P}_{SRP} is the acceleration due to the solar radiation pressure (SRP),⁹ considering Alpha as the body responsible by eclipsing the SRP during the trajectory of the spacecraft.

The equations of motion of the remaining bodies of the system are also numerically integrated along the equation of motion of the spacecraft. Since all differential equations are integrated at the same time, the initial conditions of all bodies are set for the same Epoch which is 2008, February 13th. This Epoch was used because the initial conditions of Alpha, Beta, and Gamma are well determined for this date. Thus, the initial conditions of the remaining bodies were taken from the JPL HORIZONS System* for this Epoch. Additional considerations about the initial time of integration and the PI method will be done in the next section.

We assume that Beta and Gamma are mutually disturbed and also disturbed by the gravitational potential of Alpha, but they are not disturbed by the Earth, Mars, Jupiter, the Sun, and by the solar radiation pressure. The equations of motion for Beta and Gamma are:

$$\ddot{\mathbf{r}}_{body} = -\frac{G(M_\alpha + M_{body})}{|\mathbf{r}_{body}|^3} \mathbf{r}_{body} + G \sum_{j=1}^{N-1} M_j \left(\frac{\mathbf{r}_j - \mathbf{r}_{body}}{|\mathbf{r}_j - \mathbf{r}_{body}|^3} - \frac{\mathbf{r}_j}{|\mathbf{r}_j|^3} \right) + \mathbf{P}_\alpha, \tag{3}$$

where M_{body} and \mathbf{r}_{body} are the masses and position vectors of the asteroidal moons, being $body = \beta, \gamma$. The sub-index j stands for Beta, for the equation of Gamma and vice-versa. The Earth, Mars, Jupiter, and the Sun were considered as moving in Keplerian orbits.

For all numerical simulations, we use the Runge-Kutta 7/8 integrator with variable step size. Due to the PI method, the number of points of each integration was kept in 10,000 points.

Perturbation Maps

Perturbation map is a grid of initial conditions of the spacecraft, in our case initials semi-major axis and eccentricity, in which each point is the result of the PI method over a period T of numerical integration, *i. e.*, the perturbation map reflects the result of the PI method in a map of a region constrained by the initials semi-major axis and eccentricity. Thus, the perturbation maps have the same properties of each type of the integrals in the PI method. There are four types of integrals in the PI method:

*<https://ssd.jpl.nasa.gov/?horizons>

- i. $PI_i = \frac{1}{T} \int_0^T |\mathbf{a}| dt$,
- ii. $PI_{ii} = \frac{1}{T} \int_0^T \langle \mathbf{a}, \hat{\mathbf{v}} \rangle dt$, with $\hat{\mathbf{v}} = \mathbf{v}/|\mathbf{v}|$,
- iii. $PI_{iii} = (p_x^2 + p_y^2 + p_z^2)^{1/2}$, with $p_j = \frac{1}{T} \int_0^T a_j dt$ and $j = x, y, z$,
- iv. $PI_{iv} = (p_x^2 + p_y^2 + p_z^2)^{1/2}$, with $p_j = \frac{1}{T} \int_0^T A_j dt$ and $j = x, y, z$,

where \mathbf{a} is the acceleration due to each disturber, or the summation of all disturbing accelerations, which in our case is the second, third, and fourth terms in Equation (1). \mathbf{v} is the velocity of the spacecraft, T is the final time of the numerical integration of the trajectory of the spacecraft, which can assume any value between zero and the maximum time of integration, in our case, 500 days. Precisely by the fact that T can acquire any value, the higher is the value of T , the higher is the value of the PI . For example, if we take two orbits in the same region of the system, and if this region is close to Alpha, one of these orbits can collide with Alpha and the other one not, leading to different times of simulations. From the point of view of the PI method, since its value depends on T , the orbit with no collision may have a PI greater than the orbit with collision, inducing the wrong interpretation that the orbit with no collision is more disturbed than the other one. Thus, to eliminate this distortion, we normalized the PI by introducing the factor $1/T$. $\mathbf{A} = \ddot{\mathbf{r}} - \ddot{\mathbf{r}}_{ke}$ is the difference between the total acceleration of the spacecraft, given by Equation (1), and the acceleration of a Keplerian orbit integrated along the equation of motion of the spacecraft whose initial conditions are the same of the spacecraft.

The meaning of each type of PI was defined as the method was evolved since its first appearance.⁶ The method had its beginning with the first type, the integral of the absolute value of the disturbing acceleration \mathbf{a} . The objective of that work was to measure the lunisolar perturbation over a satellite in one orbital period. The idea was that as lower the value of the PI , the less disturbed would be the orbit and as next to a Keplerian orbit the satellite would be. So the satellite would have less fuel consumption to perform a station keeping. The result of this first type of integral is the total perturbation applied to the spacecraft and it does not take into account effects that may compensate themselves during the orbit of the spacecraft. For example, the effect of the SRP can compensate itself if the spacecraft is in an orbit where the energy that the SRP takes from the spacecraft when this one is going towards the Sun is added to the spacecraft when it is moving away from the Sun. This means that the spacecraft will return to the same point where its orbit began and, for one period, the net effect of the perturbation would be zero. However, this does not imply that the orbit is not disturbed, since the trajectories with solar radiation pressure and without this effect are not the same. Thus, this type of integral allow us to compare forces with different natures.

This method have been improved in the past few years, and the other three types of integral arise from the necessity of other types of analysis. The integral of the second type shows the perturbations that affect directly the variation of energy of the spacecraft. If the value of this integral is positive, it means that the perturbation “added” energy to the small probe. In the opposite situation, the value of this type of integral is negative. Then, this type of integral is useful assess, based on the variation of energy caused by the disturbers, the stability of the spacecraft in the system. If a region in a map built with this type of integral has points with positive and negative values of PI_{ii} close to each other, this means that these orbits will take completely different paths, even with close initial conditions. This is one of the criteria used to indicate the presence of chaos. In our case, regions where there are alternating negative and positive PI_{ii} should be avoid in the Aster mission. On the

other hand, regions where there is predominant values of PI_{ii} near zero indicates the possibility of stability, since the spacecraft will neither gain energy to escape from the system nor loose energy and have its semi-major axis decreased, ending with a collision with a body of the system. In the case of orbits close to Alpha, for example, the decrease in semi-major axis that the negative values of PI_{ii} indicates a collision with Alpha itself.

The third type of integral also allows compensations of effects, since it is the integral of each component of the disturbing acceleration. This type of PI is used to identify regions more perturbed than others in a perturbation map. Regions with low values of PI_{iii} have more probability to keep the spacecraft in the system for a considerable time, since regions with high values of PI_{iii} are more perturbed, having more chance to escapes or collisions.

The fourth type of the method was idealized as a variation of the third type in References 8, 12. It measures how much a perturbed orbit deviates from a Keplerian orbit with the same initial conditions, since it measures the integral of $\mathbf{A} = \ddot{\mathbf{r}} - \ddot{\mathbf{r}}_{ke}$, where $\ddot{\mathbf{r}}_{ke}$ is the acceleration of a reference standard Keplerian orbit. The concept of this integral backs to the fundamental idea of use the integral method to perform station keeping, because this integral also measures the exact value of the Δv to be applied in an orbital maneuver to keep the perturbed orbit in the track of the Keplerian one. This is the fundamental difference from types III and IV of PI.

To analyze the stability of the orbits in the 2001 SN₂₆₃ system, it will be used perturbation maps built with PI_{iii} . To measure less disturbed orbits and to provide values of Δv required to correct an orbit to “suppress” the perturbation on it, PI_{iv} will be used. Another important point, as the concept of the perturbation maps suggest, is that they can provide the mean total velocity added to a spacecraft by a disturber or a sum of perturbations. Thus, although the Epoch used in this work is prior to the date that possibly the Aster mission will occur, the results show the mean behavior of the spacecraft and possible future state of it, no matter the initial Epoch.

RESULTS

In this section we present the results for the simulations of the grid of initial conditions of a spacecraft in the 2001 SN₂₆₃ system. Since the specifications about the size of the solar panels of the spacecraft used for the Aster mission have not yet been defined, we assume two configurations, one with a spacecraft with area-to-mass ratio of 0.02 m²/kg and the other with 0.15 m²/kg, covering two extreme configurations, since the spacecraft probably will not have mass grater than 150 kg. Thus, we separate this section in two parts, one for each area-to-mass ratio. Furthermore, in each part of this section, we compare direct and retrograde orbits.

Since the PI method works integrating the disturbing acceleration, we need a numerical method to perform this integration, after the integration of the orbit itself, where we use the Runge-Kutta method, as mentioned before. In our case, we used the Simpson 1/3 method.¹³ To ensure the desired precision to the method, we fixed the number of points for each integration of the equation of motion of the system bodies in 10,000 points.

Spacecraft with $A/m = 0.02 \text{ m}^2/\text{kg}$

We start the analysis of orbits in the system with a regular lifetime of the spacecraft map, given in Figure 1 for direct orbits and Figure 2 for the retrograde orbits. The maximum time of integration was 500 days. However, most of the orbits did not survive for this number of days, with the exception of the small region next to Alpha, between $a_0 = 1.5 \text{ km}$ and $a_0 = 5 \text{ km}$, in the retrograde map

showed in Figure 2. Thus, we cut the color bar in these two figures to 100 days, which means that all orbits in red survived for at least 100 days. The two black full circles in all figures are Gamma and Beta, respectively at $a = 3.804$ km and at $a = 16.633$ km.

We can see in Figure 1 that few orbits survived for at least 100 days. Comparing these results with Reference 4, we may conclude that the SRP wipe out almost all spacecraft from their orbits. There are regions, for example between $a_0 = 30$ km and $a_0 = 35$ km, where the lifetime of the spacecraft is almost zero. In Figure 2 we have a scenario different from Figure 1, although most of the spacecraft lifetime is also below 20 days, the number of orbits with lifetime between 20 and 60 days is greater than in Figure 1. With a more detailed look at Figure 2 we can see that the region between $a_0 = 1.5$ km and $a_0 = 5$ km, that was mentioned before, is uniform (only red dots) and does not appear in Figure 1, and they survived for the 500 days of maximum integration time.

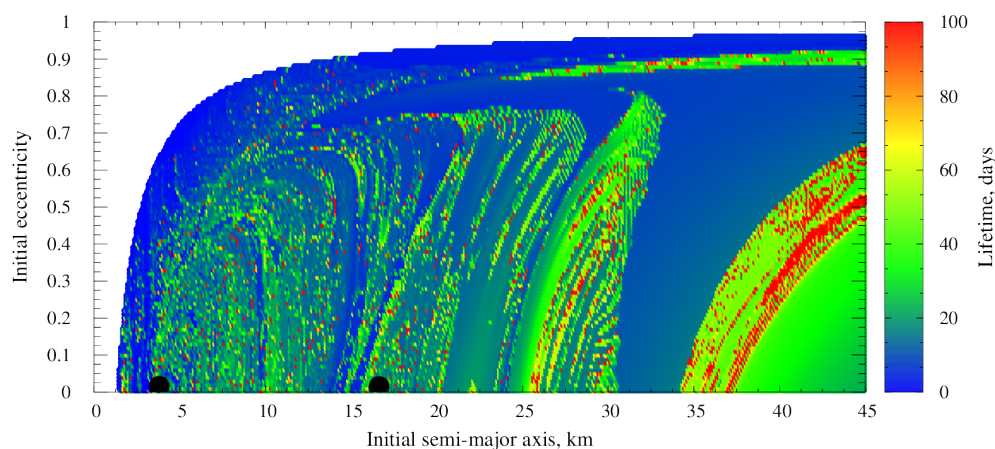


Figure 1. Lifetime of the spacecraft around the 2001 SN₂₆₃ system as a function of the initial semi-major (a_0) axis and eccentricity (e_0). Initial inclination $I = 0.001^\circ$, remaining orbital elements equal to 0° . The white region stands for orbits that escape or collided with Alpha, Beta, or Gamma. The black full circles are Gamma (at $a = 3.804$ km) and Beta (at $a = 16.633$ km). Mean area-to-mass ratio of the spacecraft equal to $0.02 \text{ m}^2/\text{kg}$.

The information coming from the lifetime maps, both retrograde and direct, are limited. Then, to determine whether a region is stable or not it is not an easy task. For example, there is a large structure between $a_0 = 25$ km and $a_0 = 45$ km, in Figure 2, that appears to be stable, since this region is populated with orbits that survive for 100 days. In this case, there will always have the necessity of integrate for more time to check if these orbits will still exist. However, by definition, the PI method can reveal instability in short period of integration, like 100 days. The thought behind this is the fact that a region that contains both positive and negative of PI_{ii} cannot be stable. To be stable, or possibly stable, a region needs to have continuous near zero values of PI_{ii} . Then, to help the understanding of some of the structures that appears in Figures 1 and 2, we will use a combination of the perturbation maps of type II and IV.

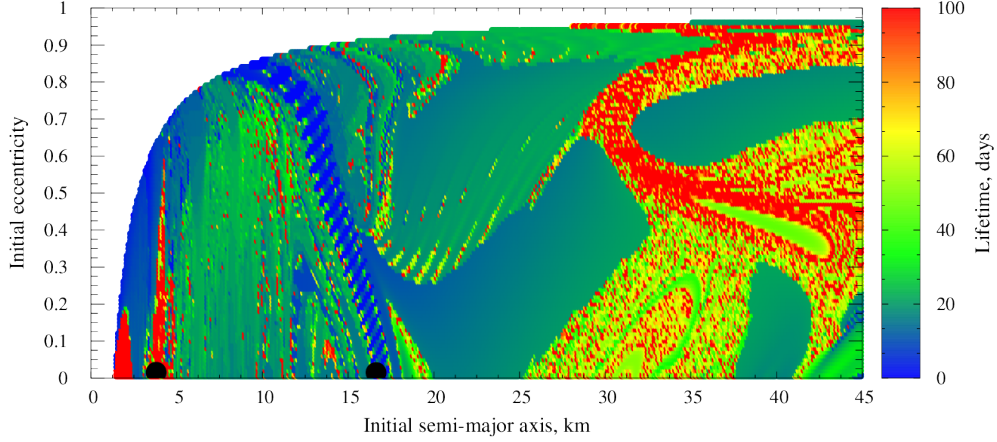


Figure 2. Lifetime of the spacecraft around the 2001 SN₂₆₃ system as a function of the initial semi-major (a_0) axis and eccentricity (e_0). Initial inclination $I = 179.999^\circ$, remaining orbital elements equal to 0° . The white region stands for orbits that escape or collided with Alpha, Beta, or Gamma. The black full circles are Gamma (at $a = 3.804$ km) and Beta (at $a = 16.633$ km). Mean area-to-mass ratio of the spacecraft equal to $0.02 \text{ m}^2/\text{kg}$.

Starting the analysis from the direct orbits, we can notice, from Figure 3, that the map of type II is divided in two distinct regimes, from $a_0 = 1.5$ km and $a_0 = 30$ km, where the surface of the map appears to be fragmented, and from $a_0 = 30$ km and $a_0 = 45$ km, where the surface of the map is smooth. In the first regime, the effects of the perturbation coming from the non-sphericity of Alpha, from Gamma and Beta are predominant. We can notice in this part of the map that there is all sort of alternation between negative and positive values of PI_{ii} , characteristics of possible chaotic behavior, as well as bands of negative and positive values, characteristic of the presence of resonances. On the other hand, in the smooth part of the map, the solar radiation pressure is dominant, almost destroying those structures. In this part of the map, the PI_{ii} is almost zero, with small fluctuations. This occurs because the net effect of the solar radiation pressure is almost zero, due to the compensations that occurs along the orbit, as mentioned before. Furthermore, PI_{ii} near zero is not enough to indicate stability of the region.

Figure 4 shows the perturbation map of type IV coming from Figure 1 (direct orbits). This map shows the balance of energy of spacecraft around 2001 SN₂₆₃ system, as a function of the initial semi-major axis and eccentricity. Since there are orbits with high values of PI_{iv} among near zero values of PI_{iv} in the same map, we cut the maximum value of PI_{iv} to show the structures that the map can present. This means that the maximum value presented in this figure, and in all perturbation maps in this work, is actually a local maximum, *i. e.*, the most disturbed orbits can not only achieve at least the value of the maximum PI_{iv} presented in the maps, but higher values than that. Analyzing the map of type IV in Figure 4, the behavior observed in Figure 3 is confirmed. The value of PI_{iv} between $a_0 = 30$ km and $a_0 = 45$ km is almost zero, but not uniform. The region is crossed by bands of low, but non-zero values of PI_{iv} . Although, from Figure 1, we can note that the lifetime in the region between $a_0 = 30$ km and $a_0 = 45$ km is 60-100 days, from Figure 4 we can notice that the Δv required to keep the orbits in this region next to an ideal Keplerian one is up to 0.02 m/s

per day. For direct orbits, this region would be the best choice for a spacecraft with $A/m = 0.02 \text{ m}^2/\text{kg}$, since there is no possible stable regions, where the use of Δv to keep the orbit as close to a Keplerian orbit as possible would be near zero, for the orbits in Figure 1. Another important observation about Figure 4 is that the region between Alpha and Gamma is heavily disturbed, since almost all orbits have $PI_{iv} = 0.08 \text{ m/s}$ per day or above this value.

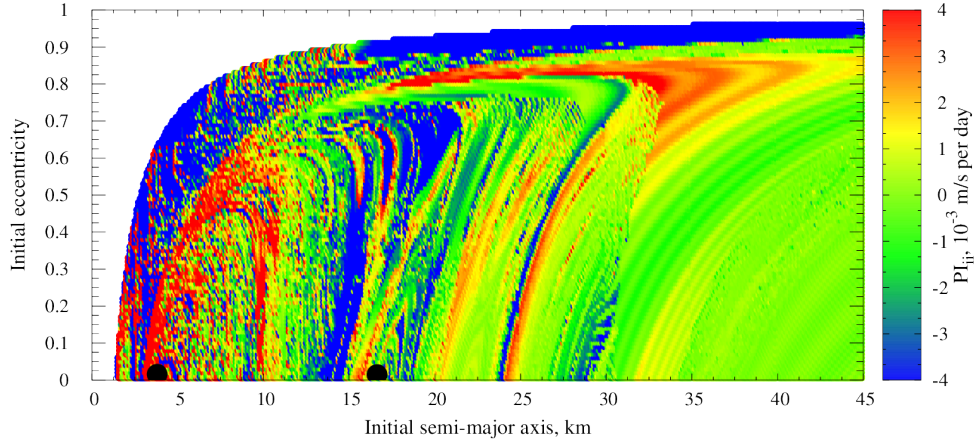


Figure 3. Perturbation map of type II coming from Figure 1 (direct orbits). This map shows the balance of energy of spacecraft around 2001 SN₂₆₃ system, as a function of the initial semi-major axis and eccentricity. $A/m = 0.02 \text{ m}^2/\text{kg}$

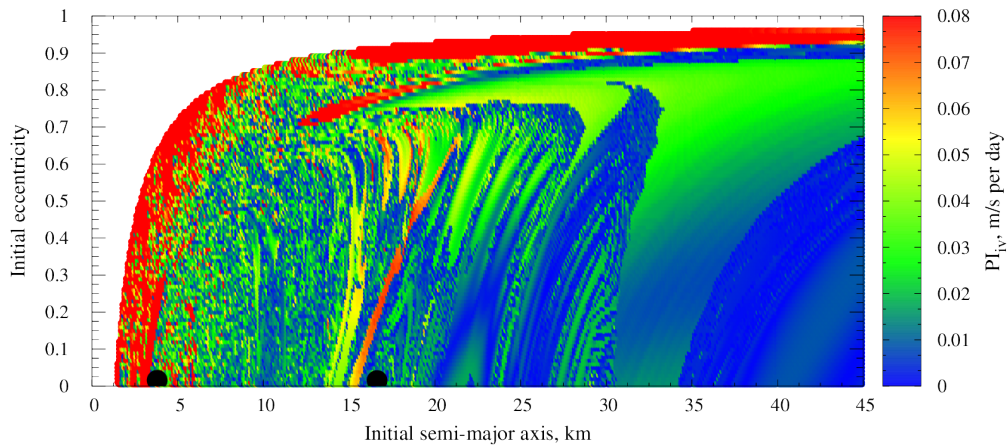


Figure 4. Perturbation map of type IV coming from Figure 1 (direct orbits). This map shows how much the particles deviates from a Keplerian orbit of reference around the 2001 SN₂₆₃ system, as a function of the initial semi-major axis and eccentricity. $A/m = 0.02 \text{ m}^2/\text{kg}$

It is well known from Celestial Mechanics that retrograde orbits are more stable than the direct

ones in the great majority of the systems, and this system follows this fact. Comparing Figure 1 with Figure 2 this fact becomes obvious by the number of orbits that survived for 100 days, but once again, there is no guarantee that the orbits that survived in Figure 2 can survive for more time of integration. Analyzing Figure 5, which is the perturbation map of type II, coming from Figure 2 (retrograde orbits), and that shows the balance of energy of the spacecraft around 2001 SN₂₆₃ system, as a function of the initial semi-major axis and eccentricity, we can see that regions where PI_{ii} is near zero are larger than the same type of region for the direct orbits. In the direct orbits, the near zero region (green area) was caused by the solar radiation pressure and we can see that because, for the direct orbits, those regions are not surrounded by negative (blue dots) and positive (red dots) values of PI_{ii} , therefore the green area is continuous. In the case of retrograde orbits, the green area is bounded by red and blue dots. This indicates a center stable for a determined period of time, surrounded by apparently chaotic motion. These characteristics indicates that the perturbation coming from the system overcomes the solar radiation pressure. These orbits are not suitable for a long term mission, because they tend to destabilize with time (with the PI_{iv} we will explain why). The role of the radiation pressure for the retrograde orbits is to change the shape of the structures in the maps, destabilizing the system. However, there is a small region between Alpha and Gamma that appears to be stable. This happens because the green region is apparently continuous, surrounded by blue and red dots, which is an analogous of an island of stability in Poincaré maps, and is close enough to Alpha for the effect of the solar radiation pressure to destabilize it. Another interesting region is a band around and above Gamma, which is probably retrograde co-orbitals with Gamma. With the map of PI_{iv} , we can check these two regions.

Figure 6 presents the perturbation map of type IV, coming from Figure 2 (retrograde orbits), that shows how much the particles deviates from a Keplerian orbit of reference around the 2001 SN₂₆₃ system, as a function of the initial semi-major axis and eccentricity. The first region to be analyzed, which is between Alpha and Gamma, is potentially stable indeed. We can see that the value of PI_{iv} is near zero and surrounded by highly disturbed orbits, which means that it is not near zero because compensational forces and the solar radiation pressure will not destabilize it. A near zero value of PI_{iv} implies that the orbit does not deviates from a Keplerian orbit of reference during the time of integration. If less disturbed, this orbit can remain stable for long periods of time with no need of orbital corrections. This region is the best candidate to place the spacecraft in this system, in retrograde orbits, with $A/m = 0.02 \text{ m}^2/\text{kg}$, since there would be no fuel consumption to keep this orbit stable. Another important point of this region is that, since the same region is unstable for direct orbits, there will be no natural particles in the way of the retrograde spacecraft.

The second region of interest in the retrograde map is the one with possible co-orbitals with Gamma. The combination of PI_{ii} and PI_{iv} near zero indicates that this region is potentially stable. This also confirms that these orbits are co-orbitals with Gamma, and not just orbits that stay for a short period of time near Gamma. In fact, the Hill's radius of Gamma is approximately 0.5 km from its center. This means that, since the Gamma radius is approximately 0.27 km, it is unlikely that the spacecraft will be captured by Gamma and even stay around it. Looking at the region around Beta, there is a large band around Beta that follows up in eccentricity. Combining observations of Figure 5 and Figure 6, we may conclude that there was temporary captures of the spacecraft by Beta, since in Figure 5 we can see that the spacecraft gain energy with respect to Alpha, which implies, since the region is confined, that the spacecraft left Alpha to orbit Beta for a short period of time. In fact, the Hill's radius of Beta is approximately 3.4 km and, being the radius of Beta equal to 0.54 km, the capture is possible. However, due to the other perturbations, as we can see in Figure 6, this capture

is temporary.

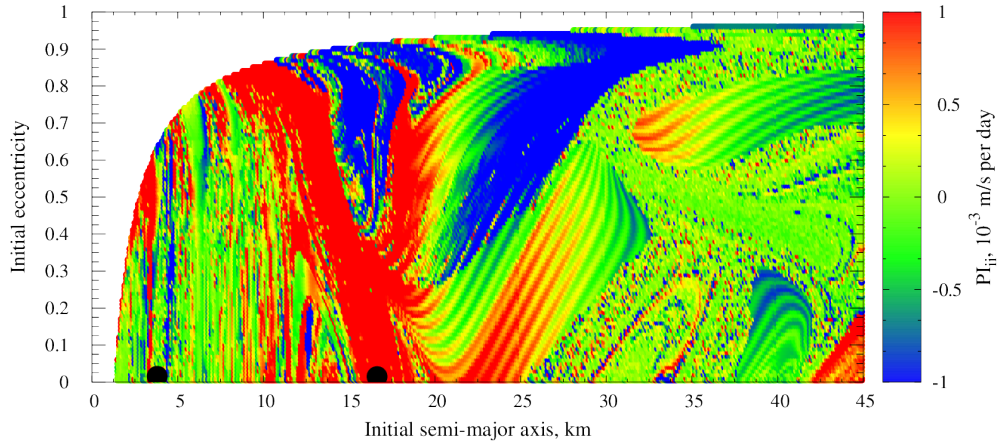


Figure 5. Perturbation map of type II coming from Figure 2 (retrograde orbits). This map shows the balance of energy of spacecraft around 2001 SN₂₆₃ system, as a function of the initial semi-major axis and eccentricity. $A/m = 0.02 \text{ m}^2/\text{kg}$

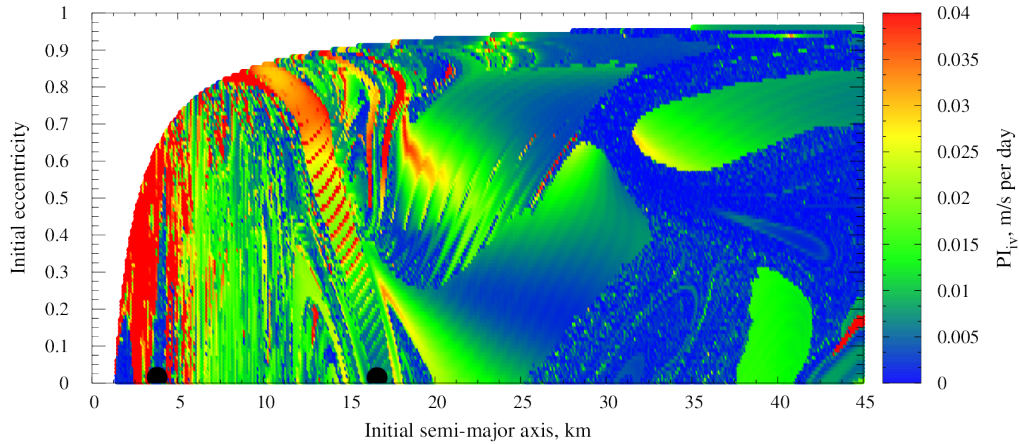


Figure 6. Perturbation map of type IV coming from Figure 2 (retrograde orbits). This map shows how much the particles deviates from a Keplerian orbit of reference around the 2001 SN₂₆₃ system, as a function of the initial semi-major axis and eccentricity. $A/m = 0.02 \text{ m}^2/\text{kg}$

The great area that have PI_{ii} near zero in Figure 5, between $a_0 = 25 \text{ km}$ and $a_0 = 45 \text{ km}$ is not stable. This fact is indicated in Figure 6, where this region does not have a uniform near zero value of PI_{iv} . This means that, although with a low value of PI_{iv} , the orbits in this region keep deviating from the Keplerian orbit of reference and eventually will, due to the solar radiation pressure, escape from the system or colliding with Alpha. However, this is still a region of interest for the mission,

because the spacecraft can stay there with the use of correction maneuvers, and the Δv required for this is given by Figure 6 and it is equal to 0.005 m/s per day for a near circular orbit with $a_0 = 35$ km.

Spacecraft with $A/m = 0.15 \text{ m}^2/\text{kg}$

Figures 7 and 8 show, respectively, the lifetime of orbits of a spacecraft with $A/m = 0.15 \text{ m}^2/\text{kg}$ in direct and retrograde orbits. For the direct orbits, the maximum lifetime decreases five times, from 100 days to 20 days and the orbits that survived for the 20 days are quite a few. These orbits are in the threshold between the influence of Alpha and the solar radiation pressure. Almost 70 percent of the orbits stayed in the system for five to 10 days. For the retrograde orbits, the behavior of the orbits is almost the same of the orbits for the direct case. The maximum lifetime is 20 days with the majority of the cases staying only up to 10 days. However, differently from the direct case, the solar radiation pressure increased the collisions with Beta. We can see it from the large band that starts in Beta and follows $a(1 - e) \approx 16.633$ km, where 16.633 km is the initial semi-major axis of Beta. The average lifetime for the direct orbits is 5 to 10 days, whereas for retrograde orbits it is 10 to 15 days. Next we will analyze Figures 7 and 8 from the point of view of the perturbation maps, starting with the direct orbits.

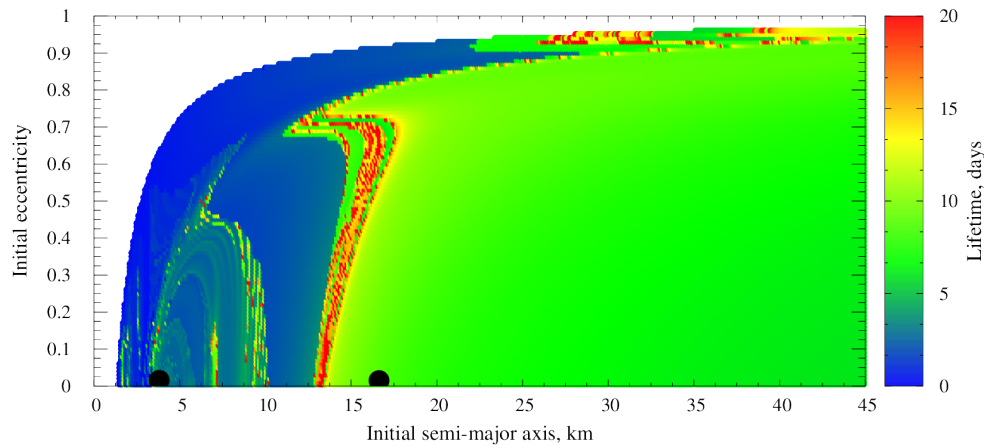


Figure 7. Lifetime of the spacecraft around the 2001 SN₂₆₃ system as a function of the initial semi-major (a_0) axis and eccentricity (e_0). Initial inclination $I = 0.001^\circ$, remaining orbital elements equal to 0° . The white region stands for orbits that escape or collided with Alpha, Beta, or Gamma. The black full circles are Gamma (at $a = 3.804$ km) and Beta (at $a = 16.633$ km). Mean area-to-mass ratio of the spacecraft equal to $0.15 \text{ m}^2/\text{kg}$.

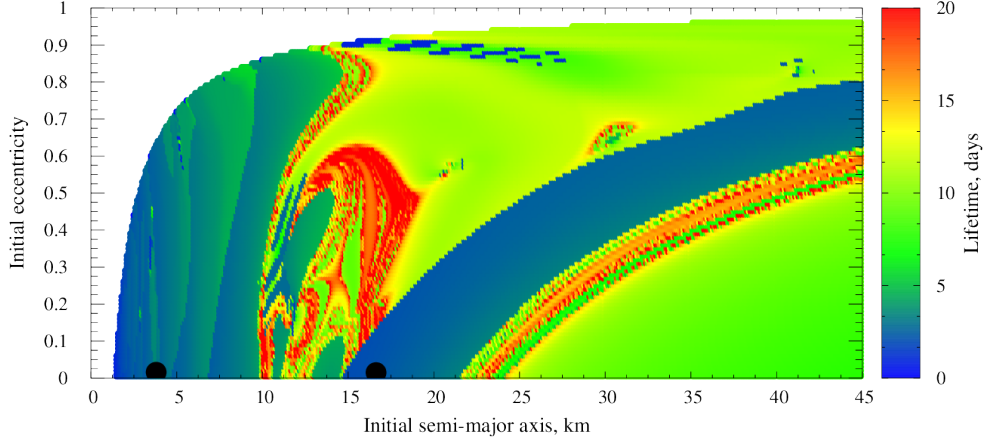


Figure 8. Lifetime of the spacecraft around the 2001 SN₂₆₃ system as a function of the initial semi-major (a_0) axis and eccentricity (e_0). Initial inclination $I = 179.999^\circ$, remaining orbital elements equal to 0° . The white region stands for orbits that escape or collided with Alpha, Beta, or Gamma. The black full circles are Gamma (at $a = 3.804$ km) and Beta (at $a = 16.633$ km). Mean area-to-mass ratio of the spacecraft equal to $0.15 \text{ m}^2/\text{kg}$.

Comparing Figures 9 and 10 we can confirm that the solar radiation pressure overcomes other effects of the dynamics of the system from $a_0 = 10$ - 15 km up to the end of the grid in $a_0 = 45$ km. In this case, the best region to place the spacecraft would be between $a_0 = 20$ km and $a_0 = 45$ km, with the consumption of fuel, in terms of Δv to keep the trajectory near Keplerian, of 0.05 to 0.15 m/s per day, given by Figure 10. Compared to the case where $A/m = 0.02 \text{ m}^2/\text{kg}$, where $\Delta v = 0.01$ m/s per day, the Δv is five times greater to keep the spacecraft with $A/m = 0.15 \text{ m}^2/\text{kg}$ in the region less disturbed.

As mentioned before, for the retrograde orbits, the solar radiation pressure tends to potencialize effects of the perturbation of Gamma and Beta. In this case, as we see in Figures 11 and 12, the useful region to place the spacecraft is constrained by $a(1 - e) \approx 25$ km, because, for $a(1 - e) < 25$ km, the effects of the asteroidal moons were increased by the solar radiation pressure. In particular, for $a(1 - e) \approx 16.633$ km, we can see in Figure 12 that the spacecraft collided with Beta, not orbiting it. Another important observation is that the region between Alpha and Gamma, where there were a stable region for $A/m = 0.02 \text{ m}^2/\text{kg}$ no longer exist for $A/m = 0.15 \text{ m}^2/\text{kg}$.

In the region $a(1 - e) > 25$ km, the Δv required to keep the orbits of the spacecraft as close as possible of a Keplerian orbit is between 0.05 and 0.1 m/s per year. If compared to the value of the spacecraft with $A/m = 0.02 \text{ m}^2/\text{kg}$ in the same region, that was 0.005 m/s per year, the new value is 10 times larger.

Due to the limitation in its size, the spacecraft for the Aster mission will have low capability of maneuver. Then, orbits that require less fuel consumption for orbital corrections are ideal for the mission. Thus, due to the effect of the solar radiation pressure in the orbits with high area-to-mass ratio, we suggest to limit the size of the solar panels of the spacecraft such that the value of the area-to-mass ratio be kept between $A/m = 0.02 \text{ m}^2/\text{kg}$ and $A/m = 0.15 \text{ m}^2/\text{kg}$. As a continuation of this work, we intend to investigate the stable region between Alpha and Gamma for retrograde

orbits for a spacecraft with $A/m = 0.02 \text{ m}^2/\text{kg}$ to verify for which values of A/m that region continue to exist.

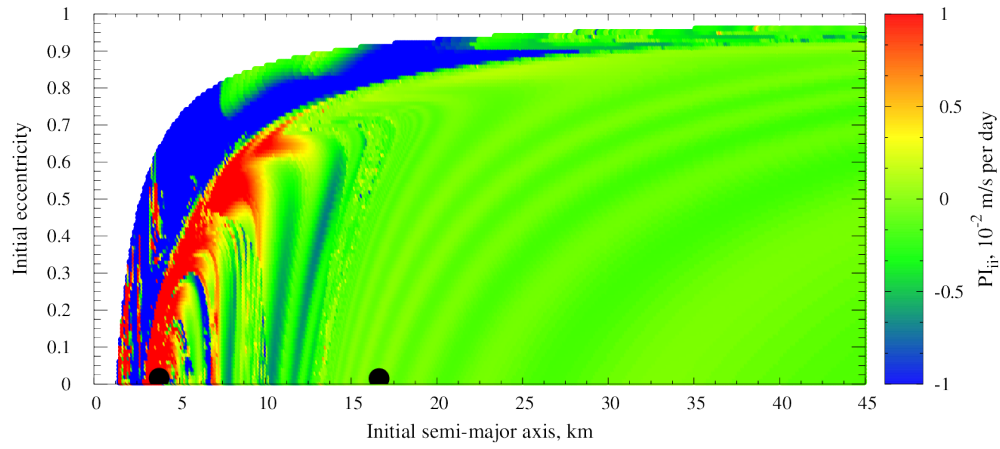


Figure 9. Perturbation map of type II coming from Figure 7 (direct orbits). This map shows the balance of energy of spacecraft around 2001 SN₂₆₃ system, as a function of the initial semi-major axis and eccentricity. $A/m = 0.15 \text{ m}^2/\text{kg}$

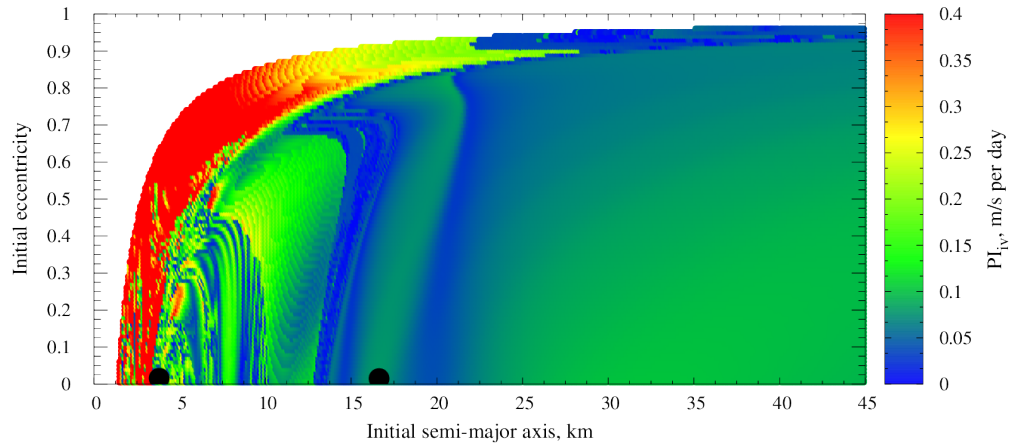


Figure 10. Perturbation map of type IV coming from Figure 7 (direct orbits). This map shows how much the particles deviates from a Keplerian orbit of reference around the 2001 SN₂₆₃ system, as a function of the initial semi-major axis and eccentricity. $A/m = 0.15 \text{ m}^2/\text{kg}$

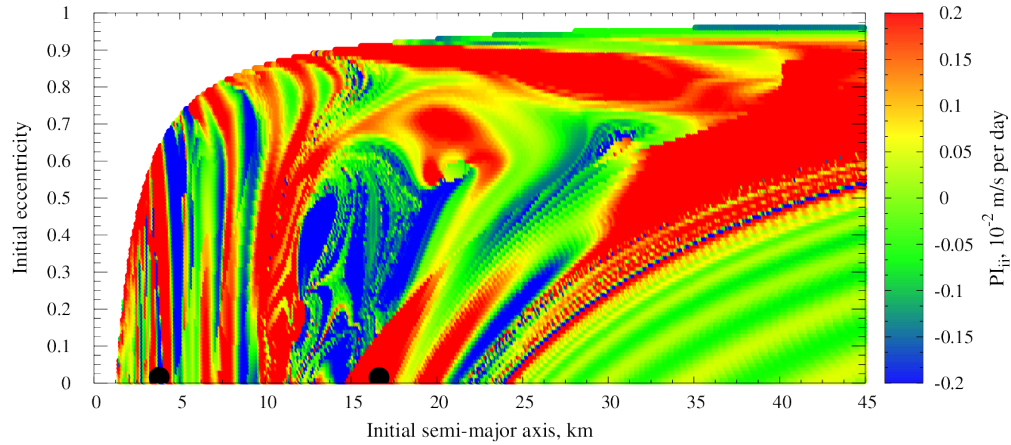


Figure 11. Perturbation map of type II coming from Figure 8 (retrograde orbits). This map shows the balance of energy of spacecraft around 2001 SN₂₆₃ system, as a function of the initial semi-major axis and eccentricity. $A/m = 0.15 \text{ m}^2/\text{kg}$

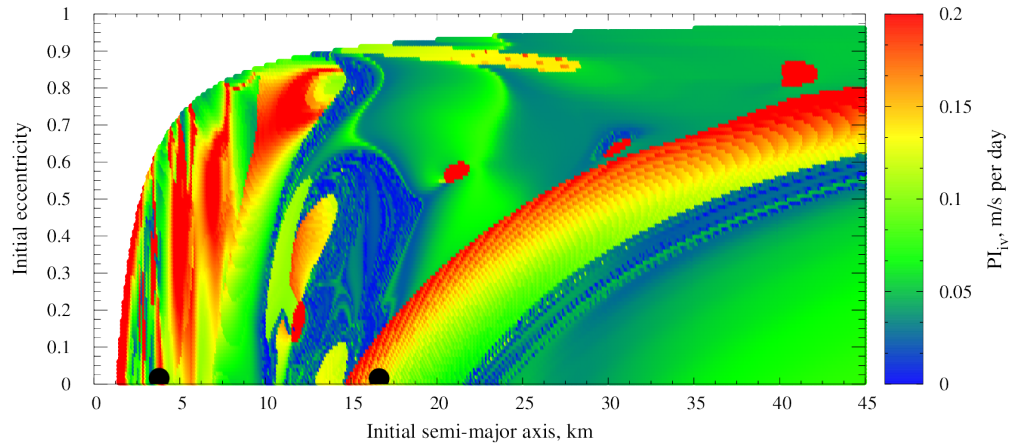


Figure 12. Perturbation map of type IV coming from Figure 8 (retrograde orbits). This map shows how much the particles deviates from a Keplerian orbit of reference around the 2001 SN₂₆₃ system, as a function of the initial semi-major axis and eccentricity. $A/m = 0.15 \text{ m}^2/\text{kg}$

CONCLUSION

The dynamics of spacecraft in the 2001 SN₂₆₃ system was investigated for direct and retrograde orbits and for two values of area-to-mass ratio, $A/m = 0.02 \text{ m}^2/\text{kg}$ and $A/m = 0.15 \text{ m}^2/\text{kg}$. The great majority of the orbits does not survived the 500 days of the maximum time of integration. In fact, for $A/m = 0.02 \text{ m}^2/\text{kg}$ the average time was 40 days with no stable area for direct orbits and 60 days with two possible stable areas for retrograde orbits. The first possible stable area, found

by the perturbation maps, is between Alpha and Gamma, and the second is a region of co-orbital orbits with Gamma. In the case of $A/m = 0.15 \text{ m}^2/\text{kg}$, the solar radiation pressure overcomes the effects of the perturbations of the other bodies of the system in the direct orbits and increased the effect of the perturbation of the bodies of the system in the retrograde case. In both cases, direct and retrograde, there is no stable regions and the maximum lifetime was 20 days.

There are regions, for both retrograde and direct orbits, that are not stable, but can be useful for the mission with the use of a Δv to correct these orbits to keep them as close as possible of an ideal Keplerian orbit. This Δv is found directly by the perturbation map built with the PI method of type IV. For $A/m = 0.02 \text{ m}^2/\text{kg}$ and direct orbits, the value of this Δv 0.01 m/s per day; for retrograde orbits, this value is 0.005 m/s per day, half of the value for the direct orbits. For $A/m = 0.15 \text{ m}^2/\text{kg}$ and direct orbits, the value of Δv is five times the value of the Δv for $A/m = 0.02 \text{ m}^2/\text{kg}$, and ten times for retrograde orbits.

The spacecraft for the Aster mission have low capability of maneuver due to the limitation in its size. Then, orbits that require less fuel consumption for orbital corrections maneuvers are ideal for the mission. Thus, due to the effect of the solar radiation pressure in the orbits with high area-to-mass ratio, we suggest to limit the size of the solar panels of the spacecraft such that the value of the area-to-mass ratio be kept between $A/m = 0.02 \text{ m}^2/\text{kg}$ and $A/m = 0.15 \text{ m}^2/\text{kg}$. As a continuation of this work, we intend to investigate the stable region between Alpha and Gamma for retrograde orbits for a spacecraft with $A/m = 0.02 \text{ m}^2/\text{kg}$ to verify for which values of A/m that region continue to exist.

ACKNOWLEDGMENT

The authors wish to express their appreciation for the support provided by grants # 301338/2016-7 and 406841/2016-0 from the National Council for Scientific and Technological Development (CNPq) and grants # 2014/22295-5, 2016/14665-2, and 2016/24561-0 from São Paulo Research Foundation (FAPESP) and the financial support from the National Council for the Improvement of Higher Education (CAPES).

REFERENCES

- [1] A. A. Sukhanov, H. F. d. C. Velho, E. E. Macau, and O. C. Winter, "The Aster Project: Flight to a Near-Earth Asteroid," *Cosmic research*, Vol. 48, No. 5, 2010, pp. 443–450.
- [2] J. Fang, J. Margot, M. Brozovic, M. C. Nolan, L. A. M. Benner, and P. A. Taylor, "Orbits of near-Earth asteroid triples 2001 SN263 and 1994 CC: properties, origin, and evolution," *The Astronomical Journal*, Vol. 141, No. 154, 2011.
- [3] T. M. Becker *et al.*, "Physical modeling of triple near-Earth Asteroid (153591) 2001 SN₂₆₃ from radar and optical light curve observations," *Icarus*, Vol. 248, 2015, pp. 499–515.
- [4] R. A. N. Araujo, O. C. Winter, A. F. B. A. Prado, and A. Sukhanov, "Stability regions around the components of the triple system 2001 SN263," *Monthly Notices of the Royal Astronomical Society*, Vol. 423, 2012, pp. 3058–3073.
- [5] R. A. N. Araujo, O. C. Winter, and A. F. B. A. Prado, "Stable retrograde orbits around the triple system 2001 SN263," *Monthly Notices of the Royal Astronomical Society*, Vol. 449, 2015, pp. 4404–4414.
- [6] A. F. B. A. Prado, "Searching for Orbits with Minimum Fuel Consumption for Station-Keeping Maneuvers: An Application to Lunisolar Perturbations," *Mathematical Problems in Engineering*, Vol. 2013, 2013, pp. 1–11. Article ID 415015.
- [7] A. F. B. A. Prado, "Mapping Orbits Around the Asteroid 2001SN263," *Advances in Space Research*, Vol. 53, No. 5, 2014, pp. 877–889.
- [8] M. Lara, "Equivalent Delta-V per Orbit of Gravitational Perturbations," *Journal of Guidance, Control, and Dynamics*, Vol. 39, No. 9, 2016, pp. 2156–2161.
- [9] O. Montenbruck and E. Gill, *Satellite orbits*. Germany: Springer, 1 ed., 2001.

- [10] D. Sanchez, A. F. B. A. Prado, and T. Yokoyama, "On the effects of each term of the geopotential perturbation along the time I: Quasi-circular orbits," *Advances in Space Research*, Vol. 54, No. 6, 2014, pp. 1008–1018.
- [11] G. Balmino, "Gravitational Potential Harmonics from the Shape of an Homogeneous Body," *Celestial Mechanics and Dynamical Astronomy*, Vol. 60, 1994, pp. 331–364.
- [12] A. K. d. Almeida, A. F. B. d. Almeida Prado, R. V. d. Moraes, and M. Lara, "Analyzing "integral indices" to quantify the effects of a perturbing force in the harmonic and Duffing oscillators," *Computational and Applied Mathematics*, Jul 2017, 10.1007/s40314-017-0471-8.
- [13] R. L. Burden and J. D. Faires, *Numerical analysis*. USA: Cengage Learning, 9 ed., 2010.